

# Dynamo action in complex flows: the quick and the fast

STEVEN M. TOBIAS<sup>1</sup> AND FAUSTO CATTANEO<sup>2</sup>

<sup>1</sup>Department of Applied Mathematics, University of Leeds, Leeds LS2 9JT, UK

<sup>2</sup>Department of Astronomy and Astrophysics and The Computation Institute, University of Chicago, Chicago, IL 60637, USA

(Received 20 July 2006 and in revised form 20 December 2007)

We consider the kinematic dynamo problem for a velocity field consisting of a mixture of turbulence and coherent structures. For these flows the dynamo growth rate is determined by a competition between the large flow structures that have large magnetic Reynolds number but long turnover times and the small ones that have low magnetic Reynolds number but short turnover times. We introduce the concept of a quick dynamo as one that reaches its maximum growth rate in some (small) neighbourhood of its critical magnetic Reynolds number. We argue that if the coherent structures are quick dynamos, the overall dynamo growth rate can be predicted by looking at those flow structures that have spatial and temporal scales such that their magnetic Reynolds number is just above critical. We test this idea numerically by studying 2.5-dimensional dynamo action which allows extreme parameter values to be considered. The required velocities, consisting of a mixture of turbulence with a given spectrum and long-lived vortices (coherent structures), are obtained by solving the active scalar equations. By using spectral filtering we demonstrate that the scales responsible for dynamo action are consistent with those predicted by the theory.

---

## 1. Introduction

Magnetic fields are ubiquitous in astrophysics and are believed to be generated by hydromagnetic dynamo action (Parker 1979). There are two fundamental questions that are addressed by dynamo theory: one is linear (kinematic) and is concerned with the nature of the dynamo growth rate for a given flow. The other is nonlinear (dynamic) and seeks to determine the amplitude of the generated magnetic field. In most cases the presence of magnetic fields is associated with turbulent flows. This has led to the idea that turbulence and dynamo action go hand-in-hand. In particular, in the kinematic case which is the subject of this paper, it has led to the belief that there is a straight-forward relationship between the statistical properties of the turbulence, as described by its spectrum function, and the dynamo growth rate (Batchelor 1950; Saffman 1963; Kraichnan & Nagarajan 1967). For the idealized case of a completely random flow this is probably true (Kazantsev 1968; Vainshtein & Kichatinov 1986). However most turbulent physical flows are not completely random. High-Reynolds-number flows can be complicated and consist of a superposition of random motions and coherent structures. The random eddies are characterized by motions on many different spatial scales with different characteristic lifetimes and turnover times whilst the coherent structures are typically stable long-lived elements in the flow (such as vortex tubes) that contain non-trivial phase information. Often

the coherent structures themselves occupy a wide range of spatial and temporal scales. The ‘ratio’ of coherent structures to random eddies in a turbulent flow varies depending on the context; geophysical and astrophysical flows that are influenced by rotation and stratification tend to be dominated by coherent structures whilst laboratory flows such as grid turbulence have a large random component and the coherent structures are more intermittent. It is natural to speculate which aspects of the turbulent flow are most important for dynamo action, which scales of motion determine the dynamo growth rate and what is the typical scale of a turbulence-generated magnetic field. Moreover does the presence of coherent structures modify the dynamo properties of the turbulence?

In this paper we argue that in those circumstances where the flow consists of a superposition of random turbulence and coherent structures the kinematic dynamo properties can be controlled by the coherent structures. Since the latter are not adequately described by the velocity spectrum, knowledge of the spectrum alone is not enough to determine the dynamo properties. What is needed is to relate the dynamo action to some other characterization of the flow that better takes into account the presence of the coherent structures. In this paper we demonstrate that in certain circumstances this can be achieved; we discuss the general theory and we illustrate this procedure for a certain class of flows.

The paper is organized as follows. In the next section we set up the theory and introduce the concept of a ‘quick dynamo’ which is central in the development of the theory. In §3 we formulate a numerically tractable problem by considering 2.5-dimensional dynamo action (i.e. dynamo action driven by a flow that is invariant in one direction). We also describe a method for generating a complex velocity field with both a random component and coherent structures using the active scalar equations. In §4 we describe the hydrodynamic properties of the resulting velocity fields for different choices of the parameters and forcing functions. The associated dynamo properties for these flows are described in §5. In §6 we verify the theory derived in §2 by considering a dynamo driven by a filtered velocity that only contains a certain range of scales. Concluding remarks are contained in §7.

## 2. Turbulent dynamos – a phenomenological model

### 2.1. *Quick dynamos*

Much of what is known about dynamo action is related to the case where the velocity has a single spatial scale. These velocities are characterized by a single magnetic Reynolds number  $Rm = U\ell/\eta$  where  $U$  is the characteristic velocity and  $\ell$  is the length scale of the flow. For these flows, dynamo action sets in if  $Rm$  exceeds some critical value. If the magnetic Reynolds number is then increased the dynamo growth rate increases and then we distinguish two different behaviours. Dynamos where the growth rate remains bounded away from zero as  $Rm \rightarrow \infty$  are termed ‘fast dynamos’ – otherwise they are termed ‘slow dynamos’ (see figure 1). The physical basis for this distinction is that slow dynamos rely on diffusion to operate whereas fast dynamos do not. As we shall see presently, in order to describe dynamos driven by velocities with a range of characteristic scales, it is useful to introduce the idea of a quick dynamo. A ‘quick dynamo’ is one that reaches a neighbourhood of its maximal growth rate quickly as a function of  $Rm$  (as shown in figure 1*b*). In other words the ascent of the growth rate is very steep, unlike the ‘pedestrian dynamo’ also shown in figure 1*b*. Note that quick dynamos may be either fast or slow and examples of both are given in figure 1(*a*): the categorization of a dynamo as quick relies on the behaviour of the

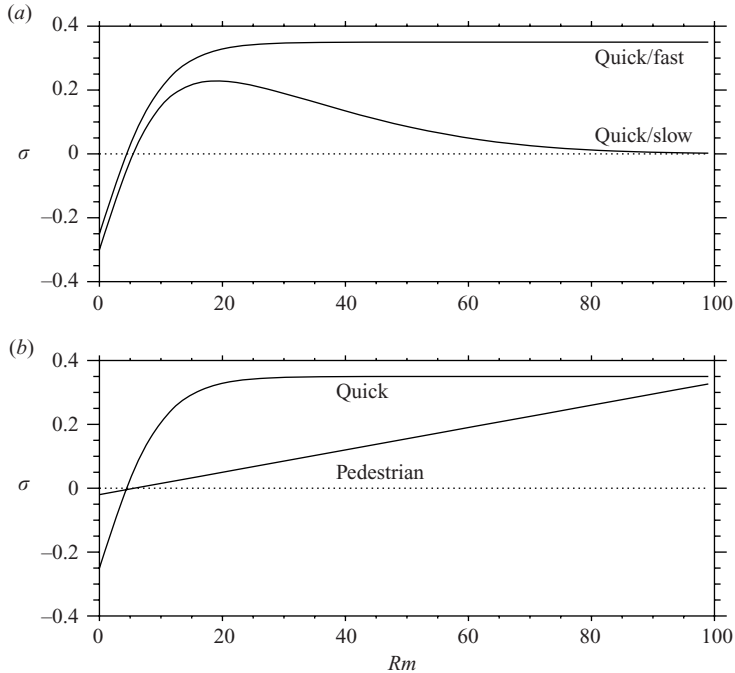


FIGURE 1. Schematic of growth rate  $\sigma$  as a function of  $Rm$  for a range of dynamos. (a) An example of a fast dynamo (with the growth rate given by equation (2.5)) and a slow dynamo where the growth rate tends to zero as  $Rm \rightarrow \infty$ . (b) An example of a ‘quick’ dynamo where the growth rate approaches its maximal value at a value close to its critical value and a ‘pedestrian’ dynamo where the growth rate is an extremely weak function of  $Rm$ .

growth rate for values of  $Rm$  a little larger than the critical one and has nothing to do with the behaviour of the growth rate as  $Rm \rightarrow \infty$ . It is important to note that the natural unit for the dynamo growth rate is the inverse turnover time of the velocity field, which for flows that exist on only one spatial scale is a well-defined quantity.

How can one adapt some of these ideas to a complex flow which, as discussed above, is characterized by eddies and coherent structures on many spatial scales with different *scale-dependent* turnover times and magnetic Reynolds numbers? Consider for example the case where the velocity has an inertial range with a spectrum that is characterized by a power law of the form

$$E(k) \sim k^{-p}. \quad (2.1)$$

To fix ideas, the most famous example is Kolmogorov turbulence for which  $p = 5/3$ . It is easy to verify that the velocity difference over a distance  $k^{-1}$  scales as

$$v(k) \sim k^{-\alpha}, \quad (2.2)$$

where  $\alpha = (p - 1)/2$ . Progress can now be made by defining the local (i.e. on a scale  $k^{-1}$ ) magnetic Reynolds number ( $Rm(k)$ ) and turnover time ( $\tau(k)$ ) to be

$$Rm(k) \sim k^{-(\alpha+1)} \sim k^{-(p+1)/2}, \quad (2.3)$$

$$\tau(k) \sim k^{-(1-\alpha)} \sim k^{-(3-p)/2}. \quad (2.4)$$

Thus it can be seen that for physically realistic values of  $p$  (i.e.  $-1 < p < 3$ ) both the magnetic Reynolds number and the turnover time decrease as the spatial scale gets

smaller. This introduces an interesting conundrum: is the growth rate determined by the large scales which have the largest magnetic Reynolds number but the longest time scale or by the small scales with the smallest Reynolds number and the shortest time scale. Immediately it can be seen from the expressions above that the answer will depend on the slope of the turbulent spectrum  $p$  as it controls the relative amplitudes of the local magnetic Reynolds number and the turnover time. In general it will also depend on the specific properties of the velocity at every scale. However we argue that if the dynamo velocities at each scale are quick as defined in the sense above then some progress can be made towards identifying the scales that are important for dynamo action.

To be specific, consider the case where each scale in isolation acts as a quick dynamo, with dynamo action setting in at a magnetic Reynolds number of order unity and reaching a large fraction of its maximal growth rate by  $Rm \sim O(10-50)$ . This is not an unreasonable example as this type of behaviour has been found in many studies of fast dynamo action (Galloway & Proctor 1992; Otani 1993; Brummell, Cattaneo & Tobias 2001). We can model such a growth curve by setting

$$\sigma = (\sigma_{max} - \sigma_{min}) \tanh(Rm/\delta) + \sigma_{min} \quad (2.5)$$

where  $\sigma_{max}$  is the maximum growth rate,  $\sigma_{min}$  is the (negative) growth rate at  $Rm=0$  and  $\delta$  is a fitting parameter that gives the dependence of growth rate on  $Rm$ . This is in fact one of the growth curves shown in figure 1. It is now possible to calculate the growth rate of an eddy of scale  $\ell = k^{-1}$  measured in units of the inverse turnover time for the largest scales. For the specific case of the profile described by equation (2.5) this growth rate is given by

$$\sigma = A_0 k^{(1-\alpha)} \left( (\sigma_{max} - \sigma_{min}) \tanh\left(\frac{A_0 k^{-(\alpha+1)}}{\eta \delta}\right) + \sigma_{min} \right) \quad (2.6)$$

where  $A_0$  is the (constant) amplitude of the largest scale for the velocity, i.e.  $v(k=1)$ . This is shown in figure 2 for particular choices of spectral slope  $\alpha$ . Note that there is a well-defined maximum for this local growth rate at a finite  $k = k_* \neq 1$  and this identifies a special range of scales that are the fastest growing ones. It is easy to verify that the condition for this curve to have such a turning point is  $\alpha < 1$  ( $p < 3$ ) which is exactly the condition for the velocity to be rough $\dagger$  (and indeed for the turnover time to be a decreasing function of  $k$  as described above). This curve clearly describes the growth rate of an eddy at spatial scale  $\ell = k^{-1}$  acting in isolation. How does this relate to the dynamo properties of a flow that is made up of a collection of eddies operating on a wide range of spatial scales? If there is no interaction at all between the dynamo properties of the eddies at different scales then the curve immediately identifies which eddy is responsible for the generation of magnetic field in the turbulent ensemble of eddies and the maximum in the growth rate is that of the corresponding magnetic field. If, on the other hand, the scales interact significantly then the curve may be of little value and the dynamo properties of the full velocity field must be considered. At the moment there is no rigorous theory on the degree of interaction of dynamos operating on different scales, although some conjectures have been proposed (Cattaneo & Tobias 2005). It is therefore worthwhile to study how

$\dagger$  The roughness exponent of a velocity field can easily be defined in terms of the scaling properties of velocity differences with separation. Let  $\delta v^q(r) = \langle (|\mathbf{v}(\mathbf{x} + \mathbf{r}) - \mathbf{v}(\mathbf{x})| \cdot \mathbf{r} / |\mathbf{r}|)^q \rangle$ , where the average is, say, over the position  $\mathbf{x}$  and time. It is then possible to construct velocities with power-law scaling  $\delta v^2(r) \sim r^{2\alpha}$ , where  $\alpha$  is the roughness exponent.

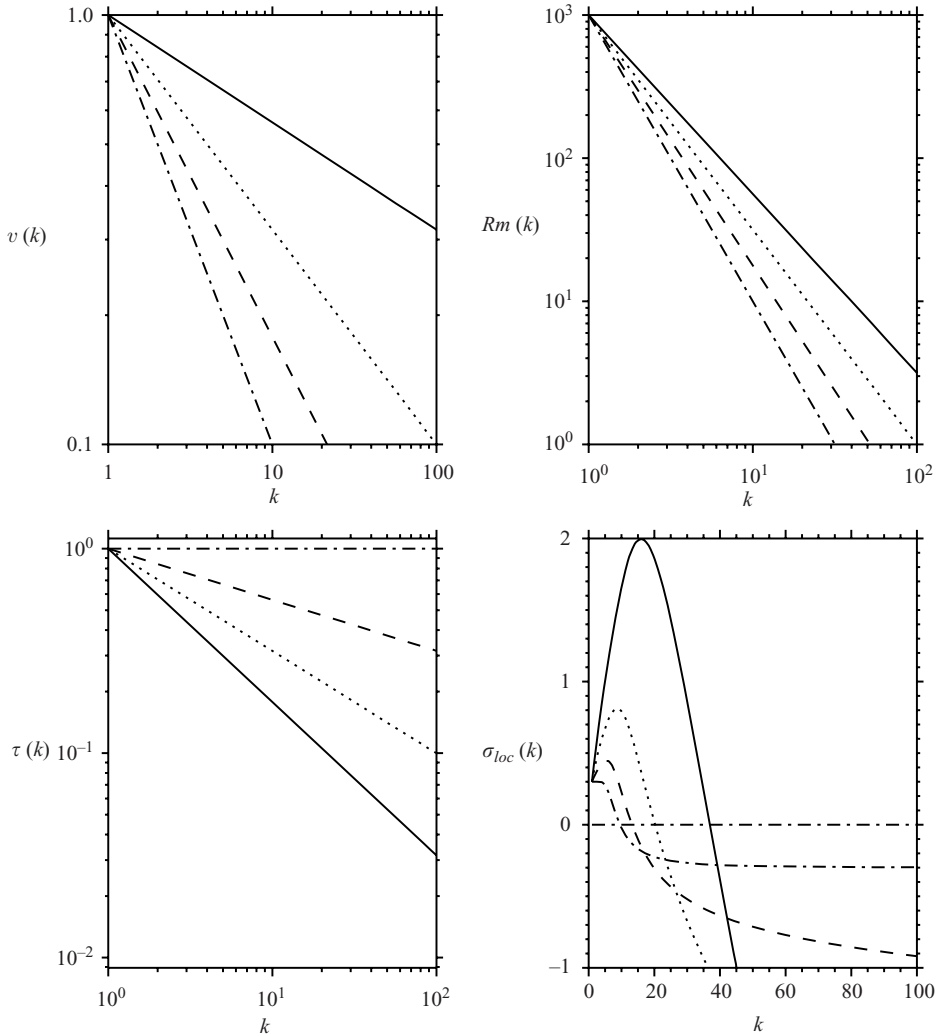


FIGURE 2. Identification of ‘local growth rates’. (a) Velocity difference  $v(k) = k^{-\alpha}$  for  $\alpha = 0.25$  (solid line),  $\alpha = 0.5$  (dotted line),  $\alpha = 0.75$  (dashed line) and  $\alpha = 1$  (dot-dash line). (b) Local magnetic Reynolds number  $Rm(k) = k^{-(\alpha+1)}$ . (c) Local turnover time of an eddy at scale  $k$   $\tau(k) = k^{-(1-\alpha)}$ . (d) Local growth rate as defined by equation (2.6).

well the heuristic argument given above describes the dynamo action of a specific example of a turbulent flow with eddies on a wide range of spatial scales.

### 3. Set-up of the model: formulation, equations and numerical scheme

There are many possible approaches to constructing a turbulent velocity of the type described in the section above, i.e. one that encompasses a wide range of spatial scales, ideally with a well-defined inertial range and non-trivial phase information that leads to the formation of dynamic coherent structures. The most natural and most realistic of these approaches is to solve the Navier–Stokes equations in three dimensions at high Reynolds number. This could be undertaken for geophysical or astrophysical flows in which the presence of rotation or stratification naturally leads

to the formation of coherent structures. Indeed some steps in this direction have been undertaken (Schekochihin *et al.* 2005). However, fully to reach the objectives set out above is extremely expensive.

For example to achieve a flow with a well-defined inertial range together with a resolved dissipative scale requires computations on the order of a few thousand spectral modes in each spatial direction. Various alternatives can be considered. One is to construct a synthetic three-dimensional velocity. This velocity then arises not through the solution of the Navier–Stokes equations, but is assembled by generating random numbers (with an amplitude determined by the required spectral slope) that are the amplitudes of the Fourier coefficients of the velocity. These spectral coefficients can be generated in such a way that the turbulent flow has well-defined turnover and correlation times. This affords some savings as now no solution of the Navier–Stokes equations is required and the induction equation may be solved in isolation. Moreover for a synthetic velocity there is no need to include the dissipative scales for the flow and this also leads to a reduction in the overall cost. However this is still a computationally expensive approach as the three-dimensional induction equation is still to be solved. In addition there is no obvious algorithm for synthesizing a velocity with non-trivial phase relations; as shown by Thomson & Devenish (2005) this can lead to significant differences between the Lagrangian statistics of the synthetic velocity relative to the Navier–Stokes velocity even when the Eulerian properties are the same. Since dynamo action is strongly influenced by the Lagrangian properties this may be cause for concern. Another possibility is to generate the velocity not as the solution of the fully resolved Navier–Stokes equations but of some large-eddy simulation (Ponty, Politano & Pinton 2004). In this case the velocity on large scales has all the desirable properties, with the saving mostly in the dissipative range. Calculations of this type, though cheaper than direct numerical simulations are still expensive (Ponty *et al.* 2005). Moreover, the filtering of the velocity in the dissipative range relies on the implicit assumption that these scales are unimportant for dynamo action. This is a particularly delicate assumption when considering dynamos at low magnetic Prandtl number where the central question is whether these scales are important or not.

From a numerical point of view, the ideal approach would be to solve the Navier–Stokes and induction equations in two dimensions, but it is well known that two-dimensional dynamo action is impossible (Zel'dovich 1957). However a compromise can be reached by considering quasi-two-dimensional dynamo action, i.e. dynamo action driven by a three-dimensional flow that only depends on two spatial coordinates, and this is the approach we shall adopt here. For flows of this type the induction equation is separable along the invariant coordinate, and so one can seek solutions for the magnetic field of the form

$$\mathbf{B} = \mathbf{b}(x, y; t)e^{ik_z z} + \text{c.c.}, \quad (3.1)$$

where c.c. stands for complex conjugate and  $z$  is the invariant direction. For any value of the wavenumber  $k_z$  the induction equation for  $\mathbf{b}$  is now two-dimensional and so extremely large values for the resolution may be achieved. This type of dynamo action has been studied by many authors, primarily in the context of flows on a single spatial scale (Roberts 1972). If the flow exhibits Lagrangian chaos then exponential stretching occurs in the  $(x, y)$ -plane. The out-of-plane component of the velocity is mostly responsible for the folding of the magnetic field. A number of velocities with these properties are believed to be good candidates for fast dynamo action (Otani 1993; Galloway & Proctor 1992).

The question still remains of how to generate a flow of the type described above, with all the properties of turbulence discussed at the start of this section. Let us consider the planar component of the flow. The natural approach would be to solve the two-dimensional Navier–Stokes equations

$$q_t + J(\psi, q) = \nu \nabla^2 q + G_z \quad (3.2)$$

where  $\nu$  is a dimensionless measure of the viscosity proportional to the inverse Reynolds number,  $G_z$  is the  $z$ -component of the applied couple,  $q(x, y, t)$  is the out-of-plane ( $z$ )-component of the vorticity,  $\psi(x, y, t)$  is the streamfunction satisfying the relation

$$q = -\nabla^2 \psi, \quad (3.3)$$

and the planar velocity is then given by  $\mathbf{u} = (u, v, 0) = \nabla \times (\psi \mathbf{e}_z)$ . The problem though is that two-dimensional turbulence is somewhat peculiar and very different to three-dimensional turbulence. The two-dimensional case is dominated by the inverse cascade of energy (McWilliams 1984). Solutions take the form of large-scale vortices with a very limited inertial range and little energy at small scales. Although the dynamo properties of interacting large-scale vortices are of interest and have been studied (Llewellyn-Smith & Tobias 2004) such flows are certainly not ideal for addressing the question posed at the end of the last section. The presence of the inverse cascade has been related to the non-locality of the Green's function for the Laplacian in two dimensions that occurs in the relationship between  $q$  and  $\psi$  given in equation (3.3). However this can be alleviated by the following 'trick' that leads to the localization of the Green's function, namely replacing equation (3.3) with

$$q = -|\nabla|^\lambda \psi, \quad (3.4)$$

with  $\lambda < 2$ . In general equation (3.4) involves fractional derivatives, the physical interpretation of which is not transparent. However the relationship between  $q$  and  $\psi$  becomes clear when considering the Fourier transform of equation (3.4) whereby

$$\hat{q}(k) = -|k|^\lambda \hat{\psi}(k), \quad (3.5)$$

where  $\hat{q}(k)$  and  $\hat{\psi}(k)$  are the Fourier transforms of  $q$  and  $\psi$  respectively and  $k$  is the modulus of the (two-dimensional) wave-vector. This system has been extensively studied (Pierrehumbert, Held & Swanson 1995; Constantin, Nie & Schörghofer 1998) for several values of  $\lambda \neq 2$ , and for  $\lambda = 1$  the resulting equations describe a physically realizable flow (Held *et al.* 1995). The equations are often termed the active scalar equations to contrast them with the case of passive scalar advection where there is no direct relationship between  $\psi$  and  $q$ . It is well known that these equations for large enough Reynolds number lead to velocities with power-law behaviour in the inertial range. The exponent of the power-law relation is controlled by the parameter  $\lambda$ . It is this property of the system that can be exploited to generate velocities with desired spectral properties, while at the same time possessing non-trivial phase relations leading to the formation of coherent structures.

The out-of-plane velocity  $w(x, y, t)$  is not set by such a procedure, but still needs to be determined. One possibility is to note that the  $z$ -component of the Navier–Stokes equations for a  $z$ -independent flow reduces to a scalar advection equation for  $w$ , namely

$$w_t + J(\psi, w) = \nu \nabla^2 w + F_z. \quad (3.6)$$

---

Case	$\lambda$	$\nu$	$k_f$	Resolution
A	2	$10^{-5}$	4	2048 <sup>2</sup>
B	1	$10^{-5}$	4	2048 <sup>2</sup>
C	1	$5 \times 10^{-6}$	100	2048 <sup>2</sup>

---

TABLE 1. Hydrodynamic velocity fields.

Hence, subject to the assumption that the forcing  $F_z = G_z$  and that  $w$  satisfies the same initial conditions as  $q$  (i.e.  $w(t=0) = q(t=0)$ ),  $w$  remains equal to  $q$  for all times. This suggests that a reasonable choice is to set  $w = q$  for all times.

We conclude this section by summarizing the strengths and weaknesses of utilizing the velocity described above as a test of the theory derived in §2. It is certainly advantageous that the velocity can be solved for in two dimensions allowing a vast range of spatial scales to be kept. This is particularly important when studying dynamos in the limit of small magnetic Prandtl number where both large scales and scales much smaller than the dissipative cutoff for the magnetic field must be kept. A further advantage is that the procedure yields structure with a long Lagrangian correlation time. Weaknesses of the procedure adopted include the independence of the velocity field of the  $z$ -coordinate and the assumption that the flow field is helical ( $w = q$ ), both of which may be thought of as promoting dynamo action. We believe however that these assumptions do not affect the main conclusions of the paper and we note that it is the coherent structures that best promote dynamo action that will win out in any flow. For example in compressible convection dynamos, magnetic field is preferentially generated by long-lived coherent elongated plumes where the vertical velocity is correlated with the vertical vorticity.

#### 4. The generation of the velocity field

The velocity field is generated in a periodic domain  $0 \leq x, y < 2\pi$  by solving the equations (3.2)–(3.4). The two-dimensional periodicity of the domain suggests the implementation of pseudo-spectral techniques, which are extremely efficient for nonlinear advection diffusion problems. Furthermore this affords the added simplification that the relationship given by equation (3.4) is easily implemented by imposing its analogue in spectral space, namely equation (3.5).

We have generated three velocity fields for the values of the parameters shown in table 1. In all cases the forcing takes the form  $G_z = G_0 \cos k_f x \cos k_f y$  with  $G_0 = 0.1$ . The calculations were started from static and integrated until a statistically steady turbulent state was achieved, in which the ‘enstrophy’ (i.e.  $q$ ) spectrum has converged (cf. Pierrehumbert *et al.* 1995). Figure 3 shows density plots of  $q$  for the three cases at a representative instant. Following common practice we illustrate the solutions by showing  $q$ . However we note that the physical interpretation of these pictures requires some care. For  $\lambda = 2$  (figure 3a),  $q$  does represent the vertical vorticity, whereas for  $\lambda = 1$  (figures 3b, c)  $q$  has no obvious physical meaning – although it does have the dimensions of a velocity. The importance of the parameter  $\lambda$  can be understood by first comparing figures 3(a) and 3(b). In Case A, which is two-dimensional Navier–Stokes turbulence, the solution is dominated by the presence of two vortices with opposite circulation, with filamentary vortex sheets in between. In contrast case B, which still has large-scale vortices, has coherent structures on a wide range of spatial scales in the intervening space. These secondary smaller vortices are the result of an instability



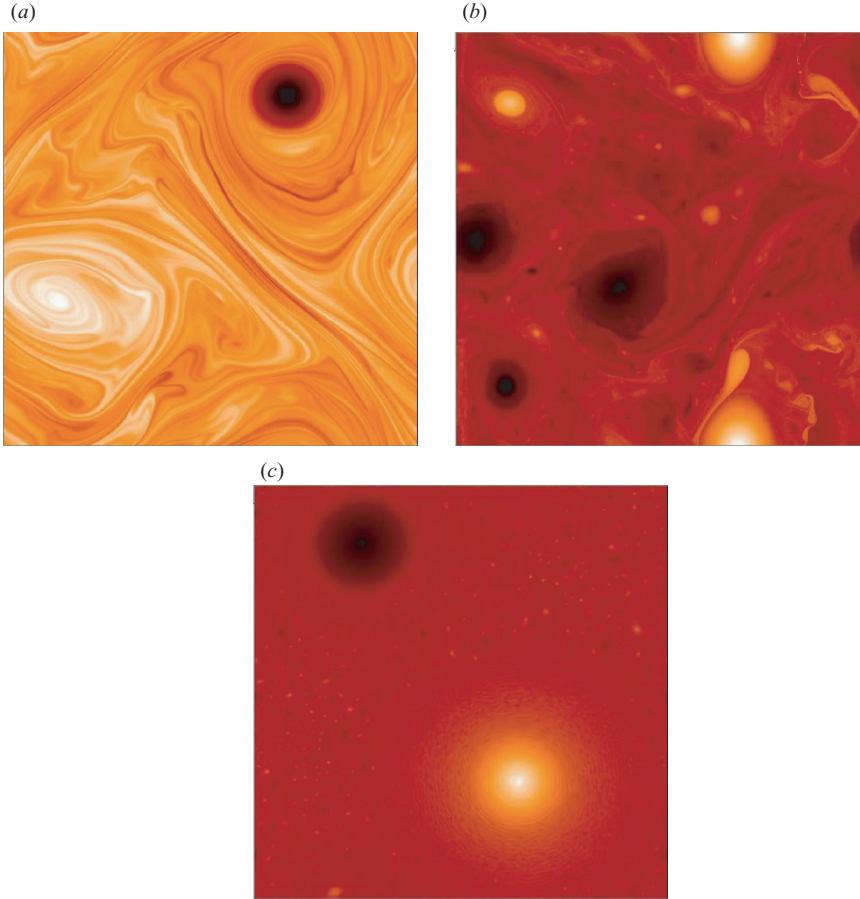


FIGURE 3. Density plots for  $q(x, y)$  at a representative time in the evolution. (a) Case A where  $\lambda=2$  and  $k_f=4$  – this case corresponds to regular two-dimensional Navier–Stokes; (b) Case B  $\lambda=1$ ,  $k_f=4$  (large-scale forcing with a forward-cascade); (c) Case C with  $\lambda=1$ ,  $k_f=100$  (small-scale forcing with an inverse-cascade).

of the vortex sheets. This instability becomes more pronounced as  $\lambda$  decreases: as  $\lambda$  decreases the velocity becomes more spatially localized relative to the vorticity and so a given shear profile becomes more unstable (Pierrehumbert *et al.* 1995). Figure 3(c) also shows large-scale vortices and fine-scale structure. However the physical nature of this solution is completely different. In Case B (which is driven at large scales) the small-scale structure arises as a consequence of the series of instabilities described above resulting in a forward cascade. For Case C it is the small-scale structures that are driven by the forcing directly and the large-scale structures are the result of an inverse cascade. These differences are manifested in the  $q$ -spectra, which are shown in figure 4. Figure 4(a) shows the spectrum for Case B; the spectrum for  $q$  shows a very large and well-defined inertial range, with a spectral index of  $-1.83$ . By contrast, in figure 4(b) for Case C the forcing wavenumber is clearly visible as well as a forward spectrum with an index of  $-2.79$  and an inverse cascade with an index of  $0.99$ . For comparison the spectrum for Case A has also been included in figure 4(a). It is clear that for this case the inertial-range scales are not described by a power law and that the small scales are not excited to the same degree as for Case B.

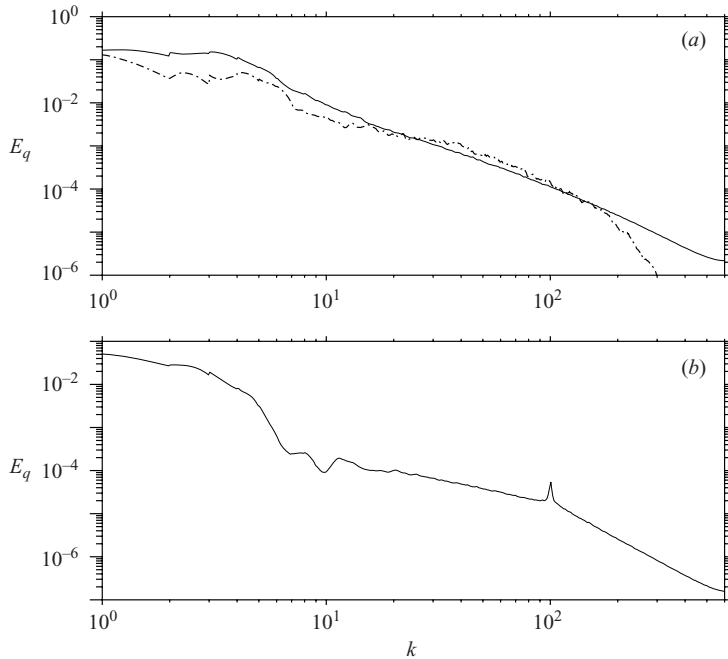


FIGURE 4. Two-dimensional spectra for  $q$  ( $E_q(k)$ ). (a) The spectrum for Case B ( $\lambda = 1$ ,  $k_f = 4$ ) – the spectrum for Case A is included (as a dot-dashed line) for comparison. (b) Case C ( $\lambda = 1$ ,  $k_f = 100$ ). For Case B a forward cascade is visible whilst for Case C both a forward and inverse cascades are found.

## 5. Dynamo properties

The dynamo properties of the velocity fields generated in the previous section are now investigated by solving the induction equation together with the evolution equation for  $q$ . As the flows are incompressible, the induction equation takes the form

$$\mathbf{B}_t + \mathbf{u} \cdot \nabla \mathbf{B} = \mathbf{B} \cdot \nabla \mathbf{u} + \eta \nabla^2 \mathbf{B}, \quad (5.1a)$$

$$\nabla \cdot \mathbf{B} = 0, \quad (5.1b)$$

where  $\eta$  is the dimensionless magnetic diffusivity related to the inverse magnetic Reynolds number. As mentioned above, the nature of the velocity allows separable solutions of the induction equation of the form (3.1) where  $k_z$  is now a parameter and should not be confused with  $k$  which is the horizontal wavenumber. Equation (5.1) is then solved as an initial value problem (with initial conditions given by a random solenoidal magnetic field) and the growth rate  $\sigma$  is determined. Figure 5 shows  $\sigma$  as a function of  $k_z$  and  $Rm$  for Cases B and C. Here and for the rest of the paper  $Rm$  is defined on the integral scale, and changes in  $Rm$  are achieved by changing the diffusivity  $\eta$ . The behaviour of the growth curve is similar for the two cases. Near the origin all the growth curves are positive and the growth rate increases with  $k_z$ , with a rate that itself increases with  $Rm$ . It is clear that for finite  $Rm$  all the growth curves must become negative for large enough  $k_z$  (as at high enough  $k_z$  vertical diffusion destroys field faster than advective processes can generate field). Hence for all curves of this type there must be at least one value of  $k_z$  for which the growth rate is maximal. However one cannot exclude the possibility that more than one such maximum exists and the curve is non-monotonic on either side of the maximum

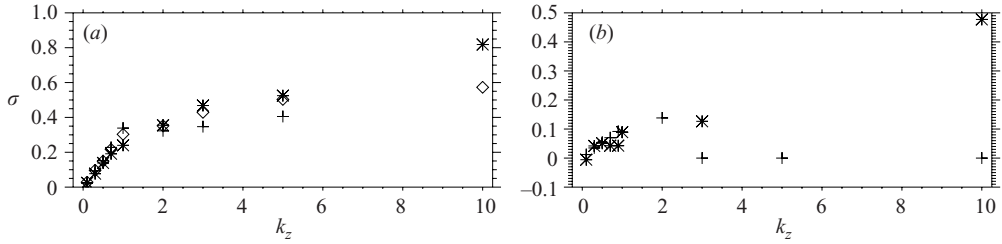


FIGURE 5. Growth rate as a function of  $k_z$  for different values of  $\eta$  and different flows. (a) The growth rate  $\sigma(k_z)$  for Case B for three different values of  $\eta$  ( $\eta=0.01$  (crosses),  $\eta=0.001$  (diamonds),  $\eta=0.0001$  (asterisks)). (b) Case C for two different values of  $\eta$  ( $\eta=0.001$  (crosses) and  $\eta=0.0001$  (asterisks)).

value. In general one also expects that the range of unstable wavenumbers increases as a function of  $Rm$ . For instance, for Flow B for  $\eta=0.001$  the growth rate becomes negative by  $k_z=6$  whereas for  $\eta=0.0001$  all the wavenumbers investigated lead to positive growth rates. For Case B (figure 5a) it is clear that as  $Rm$  is increased the mode of maximal growth rate moves to larger and larger  $k_z$ . Hence the preferred vertical scale for the magnetic field is getting smaller and smaller as  $Rm$  increases. This behaviour is different to that characterizing fast dynamos acting on one scale: for example for the Galloway–Proctor flow the preferred vertical wavenumber stays fixed at  $k_z=0.57$  as  $Rm$  is increased. This behaviour for our flows is indicative of the fact that, as  $Rm$  is increased, the length scale of the eddy that is important for the generation of magnetic field is decreasing. This is discussed further in the conclusions.

A greater understanding of the role of the turbulent eddies in generating the magnetic field can be gained by examining figure 6, which shows density plots of  $B_x$  together with the corresponding density plots for the vertical velocity  $w$  (which of course is set to the value of  $q$ ). We stress again here that for  $\lambda=1$   $q$  has the dimensions of velocity and not vorticity. Figure 6(a) shows  $w$  and  $B_x$  for Case B at a representative time in the evolution. As noted before, the velocity field takes the form of eddies on many scales (with different turnover times). The magnetic field ( $B_x$ ) also has a distinctive spatial pattern, with two main features being apparent. First, the magnetic field appears to be generated preferentially around coherent eddies of a certain size: the large eddies do not appear to be contributing much to the generation of field, but regions of strong magnetic field always seem to be associated with edges of the eddies on an intermediate scale. The second feature is that the magnetic field at the edge of intermediate eddies takes the form of long thin filaments with a characteristic width and length. Comparison of calculations at different values of  $Rm$  and  $k_z$  (not shown) demonstrates that the width of these magnetic filaments is largely controlled by  $Rm$ . Indeed, although for large enough  $Rm$  the growth rate is a weak function of  $k_z$ , there is an interesting change in the morphology of the filaments as  $k_z$  is changed: for large  $k_z$  the magnetic field has a more complicated structure in the region of strong strain with many magnetic filaments occupying this region. It is to be expected that the thickness of these filaments will scale as  $Rm^{-1/2}$ , getting thinner as  $Rm$  is increased; this change of scale for the widths of the filaments is manifested in the spectrum of the field discussed later in this section. The length of the filaments is a more complicated function of both  $Rm$  and  $k_z$ , but in general is largely insensitive to changes in  $Rm$  and a weak function of the vertical wavenumber  $k_z$ . Figure 6(b), which shows the flow and  $B_x$  for Case C, are even more striking. Here the two large

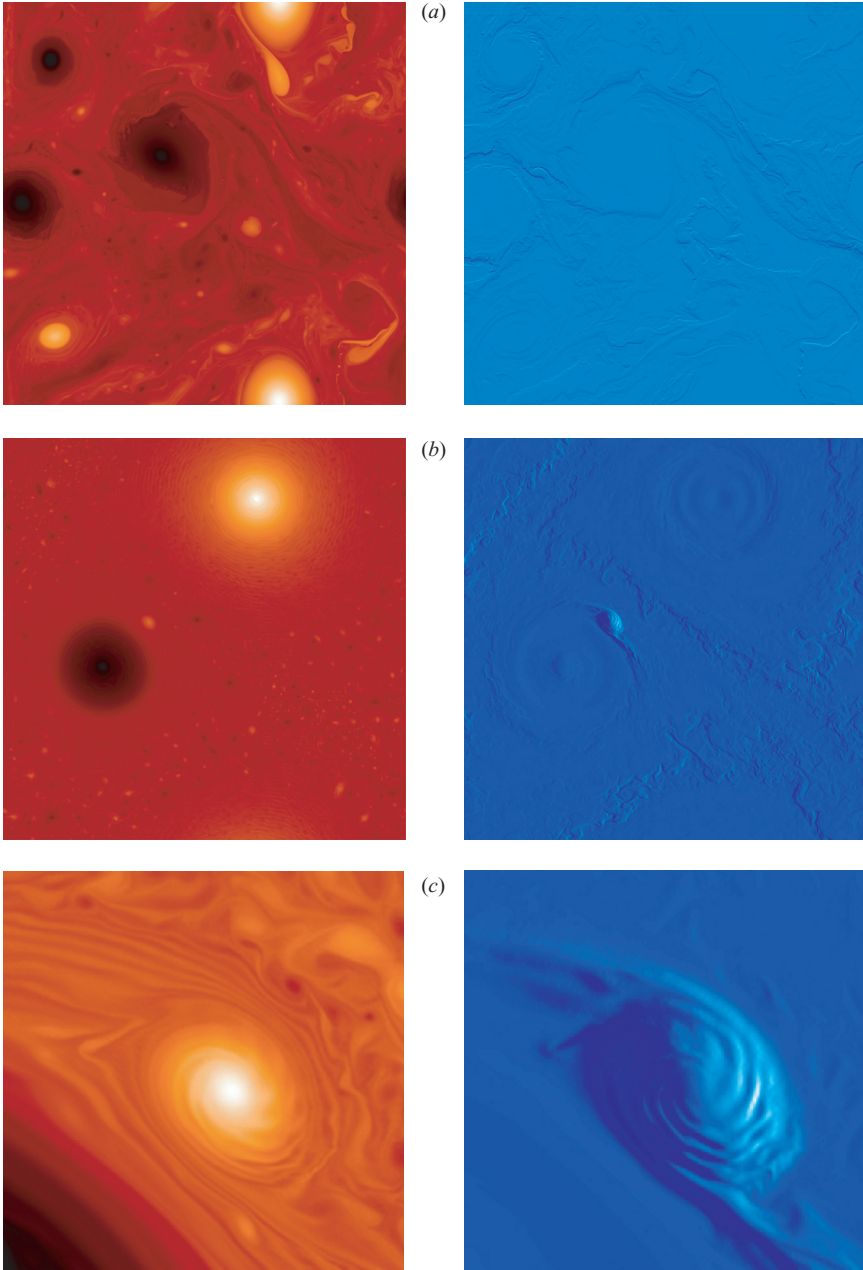


FIGURE 6. Spatial form of the dynamo magnetic field. Density plots for  $q$  (left panels) and  $B_x$  (right panels) showing the form of the magnetic field. (a) A representative point in the evolution of Case B (with  $\eta=0.0001$  and  $k_z=10$ ). (b) Case C (again with  $\eta=0.0001$  and  $k_z=10$ ). (c) A close-up of a dynamo eddy and the form of the resulting magnetic field.

vortices do not appear to be directly involved at all in the generation of the magnetic field. The magnetic field is clearly associated with eddies at an intermediate scale, with one particular eddy playing a dominant role. Note that substantial magnetic field generation is also achieved by various vortex streets of intermediate eddies between

the two main vortices. Figure 6(c) shows a close-up of the eddy that is responsible for much of the magnetic field generation and the corresponding magnetic field. This vortex appears to be very efficient at generating magnetic field, with this field taking on a distinctive spiral form. These images are entirely consistent with our picture of a preferred band of ‘active’ velocity wavenumbers being responsible for the bulk of the field generation. In this case the wavenumbers correspond to coherent vortices in the flow of a certain size, with both larger and smaller vortices appearing to contribute little to the generation process.

As noted above, complementary information can be gained about the form of the magnetic field by examining the corresponding (two-dimensional) spectra, as shown in figure 7. Here figure 7(a) shows the spectrum for the magnetic field for Case B for the two smaller values of  $Rm$  corresponding to  $\eta=0.01$  and  $0.001$ . These spectra are calculated in the following manner. When the magnetic field is growing exponentially (on average) two-dimensional spectra are calculated at a number of different times during the exponential growth. The individual spectra are then normalized (in such a manner that they take on the same value in the diffusive sub-range) so that the exponential growth has been removed. The average of the normalized spectra is then calculated and this is now representative of the typical spectral form of the eigenfunction. Typically the calculated spectrum is the average of twenty realizations. Although significant averaging has been performed, it is difficult to achieve convergence to a well-defined average at the low wavenumbers (although the averages at the high wavenumbers are certainly well converged). Figure 7(a) shows that the form of the spectrum is typical of that for kinematic dynamos of this type. There is a slight rise in the spectrum for the magnetic energy as  $k$  is increased until the scale gets close to the diffusive cutoff. At this point the energy drops rapidly as diffusion sets in. Here the difference in the value of  $\eta$  between the two curves is manifested in the scale at which the diffusive cutoff occurs. Figure 7(a) also shows for comparison the spectrum for  $q$ . It is clear from this that the diffusive cutoff for the magnetic field occurs at a much larger scale than that for the velocity field. This is exactly the regime of interest if the magnetic Prandtl number ( $Pm = \nu/\eta$ ) is small. What we have clearly demonstrated here is that the dynamo has no problem in working efficiently when its (ohmic) diffusive cutoff is in the middle of the inertial range for the velocity – we shall discuss this further in the conclusions. Figure 7(b) shows the magnetic spectrum for all three values of  $\eta=0.01, 0.001$  and  $0.0001$ , also for Case B. Again the characteristic shape of the spectrum is apparent at the highest  $Rm$ , although the diffusive cutoff has moved to higher values of  $k$ . For  $\eta=0.0001$ , the diffusive cutoff for the magnetic field is just to the left (i.e. at lower values of  $k$ ) of that for the velocity, so the dynamo is working at low (although not tiny)  $Pm$ .

## 6. Filtered dynamos

The theory of §2 described how the turbulent dynamo can be envisaged as a competition between large-scale slow eddies and smaller-scale fast eddies – the large scales are dynamos but have a long turnover time and hence a smaller growth rate whilst the small scales are not at a high enough  $Rm$  to be dynamo unstable – and how a preferred ‘active dynamo’ scale can be identified. For the example of figure 2, where the dynamo velocity field consists only of an inertial range with a well-defined spectral slope this ‘active dynamo’ scale can be identified unambiguously. This process is, however, non-trivial in a realistic turbulent flow and identification of a ‘dynamo scale’ requires some further analysis. The numerical examples of the previous section

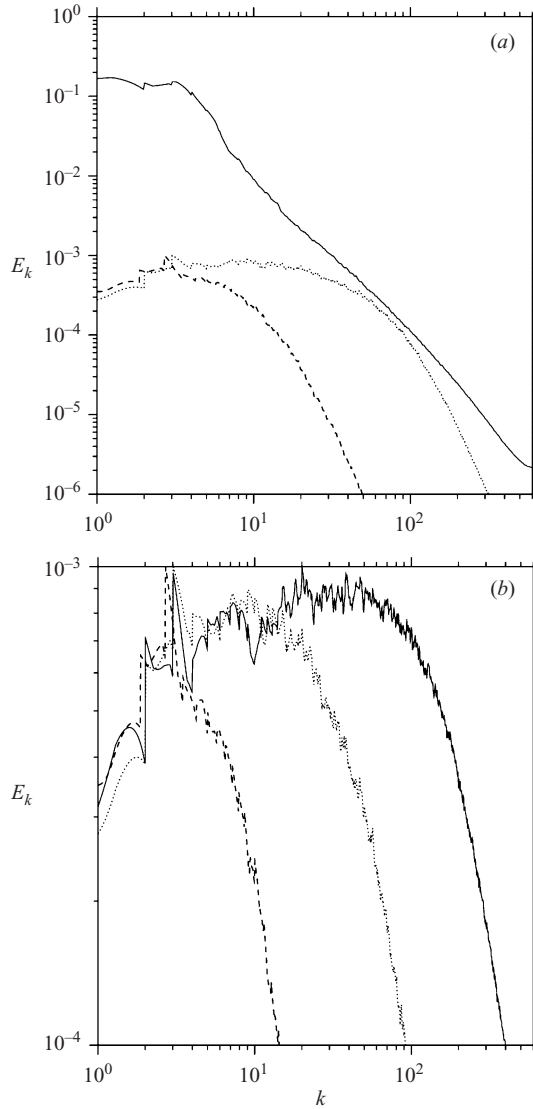


FIGURE 7. Spectra of the magnetic field for different values of  $\eta$ , corresponding to Case B with  $k_z = 10$ . (a) The spectra of the magnetic field (normalized as described in the text) for  $\eta = 0.01$  (dashed line) and  $\eta = 0.001$  (dotted line). As  $\eta$  is decreased the dissipative scale moves to the right. Shown for comparison is the spectrum of  $q$  (solid line). Note that the dissipative scale for the magnetic field lies in the inertial range of the turbulence. (b) The spectrum for the magnetic field for all three values of  $\eta = 0.01$  (dashed), 0.001 (dotted) and 0.0001 (solid).

indicate that the magnetic field generation arises as a result of the eddies in the flow of a certain spatial scale (see figure 6), eddies on a larger scale being ‘too slow’ whilst smaller eddies being ‘too weak’. The aim of this section is to formalize the general picture described above.

We claim that the figures showing magnetic field and velocity suggest that certain eddies are responsible for the generation of magnetic field in our turbulent dynamo. How is it possible to test such a claim? The ideal approach would be to take the given velocity field and simply remove the eddies that are believed to be responsible

for the growth of magnetic field. Such a procedure would invariably have a significant effect on the form and growth rate of the dynamo-generated magnetic field – with the growth rate dropping significantly as the eddies are removed. It is however impractical to remove specific eddies from a velocity field in a computationally efficient manner (although it may be possible using wavelet analysis). Instead we adopt the procedure of filtering the velocity field in spectral space in the induction equation, i.e. we still solve the full evolution equation for  $q$ , but pass the velocity through a filter before putting it into the induction equation. Hence only certain wavenumbers from the velocity are allowed to drive the growth of magnetic field. We proceed by examining how the dynamo growth rate changes for a representative dynamo as the velocity field becomes progressively more filtered. We choose as a basic dynamo state the velocity field given by Case B, and set  $\eta = 0.001$  and  $k_z = 10.0$  (as shown in figures 6 and 7). We choose to implement both a high-pass and low-pass filter on the velocity, that is we take the full velocity field as generated by the evolution equation for  $q$  and filter off either the high wavenumbers or the low wavenumbers. Examples of the velocity fields that are achieved by filtering are shown in figure 8. Figure 8(a–d) shows the effect of filtering off the low wavenumbers for four different values of the cutoff  $k_{fil}$ ; the filter adopted here is a Heaviside filter where all the modes with  $k < k_{fil}$  are set to zero. It is clear that filtering off the low wavenumbers leads to the velocity field being concentrated on smaller and smaller scales, although it is still possible to see the presence of coherent structures on small scales here. It is also possible to see the ‘ghost’ of the large-scale coherent eddies in the flow as holes in the small-scale flow. Figure 8(e)–(h) shows the corresponding velocity field when the high wavenumbers are filtered off (i.e. all modes with  $k > k_{fil}$  are set to zero). As expected filtering off the very highest wavenumbers appears to have little effect on the form of the velocity field (the wavenumbers have little energy associated with them and are on exceptionally small scales). As  $k_{fil}$  is decreased the filtering does have a noticeable effect on the form of the velocity field, with the large-scale structures becoming more blurred at the edges by the time  $k_{fil} \approx 50$ . Further decrease in the spectral cutoff leads to the successive removal of coherent structures of a given size, until only the  $k = 1$  mode is kept in each direction (bottom right panel).

We proceed by selecting these velocities as inputs for the induction equation and calculating the corresponding growth rates and generalized eigensolutions. The results are shown in figures 9 and 10. Our conjecture in §2 is that much of the dynamo growth is the result of flows (eddies) of a certain scale (in a certain band of wavenumbers). If this is the case then filtering off modes from the velocity field that are larger or smaller than this scale should have little effect on either the growth rate or the form of the generated magnetic field. It is to be expected that only when the active dynamo scales are removed from the velocity field will the growth rate and eigensolution change significantly, with the growth rate being reduced. Figure 9 shows the growth rate  $\sigma$  as a function of the cutoff  $k_{fil}$  for both the case when low wavenumbers are filtered off (a) and when high wavenumbers are filtered off (b). In this plot error bars are included in the values of the growth rate as it is difficult to calculate precisely the dynamo growth rate in filtered flows. Figure 9(a) (when the high wavenumbers are kept) should be read from the left. For  $k_{fil} = 0$  all the modes are kept and the growth rate is the same as that for the full velocity field. As  $k_{fil}$  is increased the growth rate begins to decrease slightly (but remains unchanged within the error bars) until  $k_{fil} \approx 10$ –20. For larger values of  $k_{fil}$  the dynamo growth rate is significantly reduced and the dynamo has effectively switched off by  $k_{fil} \approx 60$ . Of more interest is the behaviour demonstrated in figure 9(b) for the case where the low wavenumbers

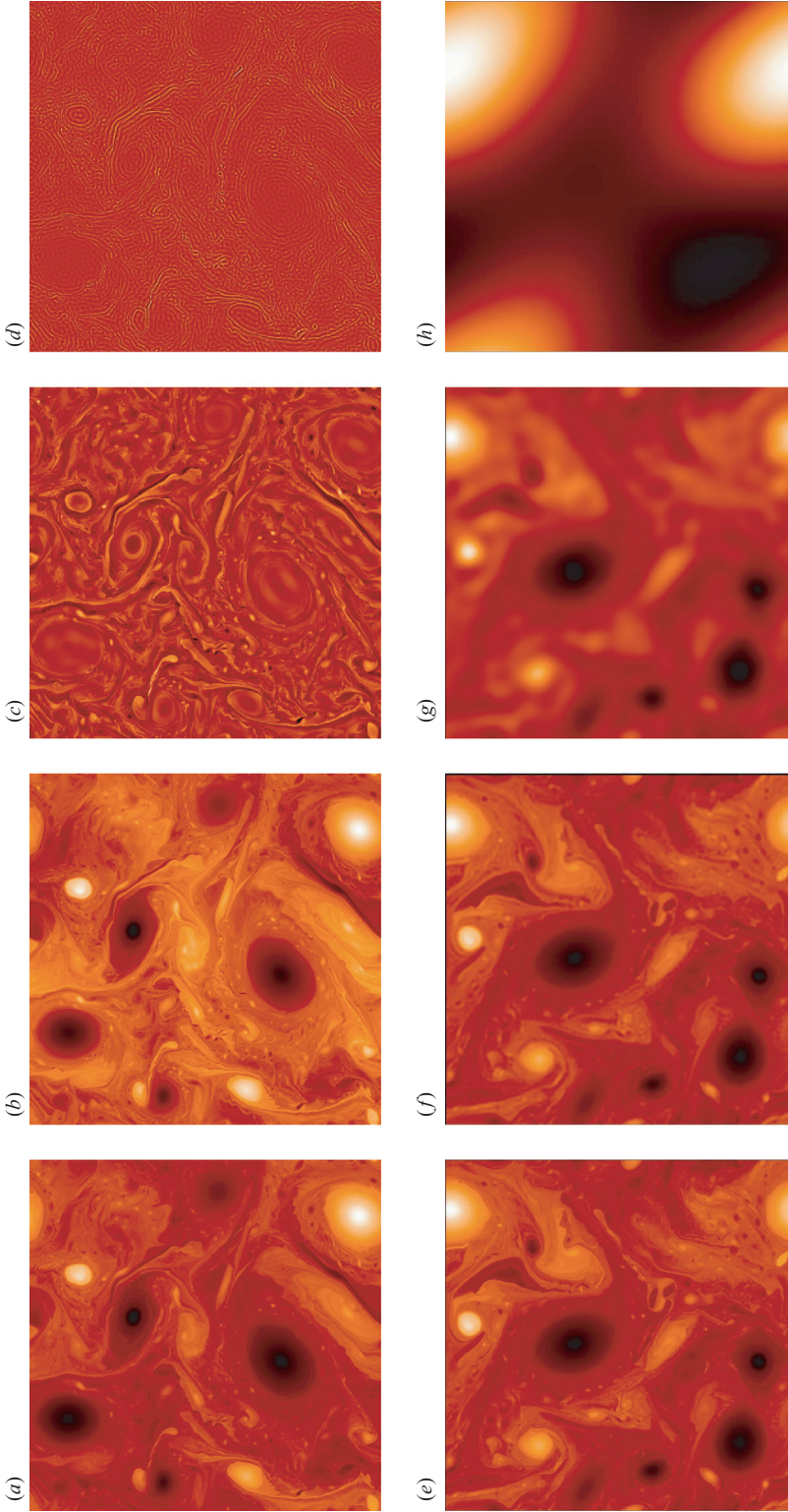


FIGURE 8. Filtered velocity fields. Density plots of the filtered vertical velocities ( $w=q$ ) at a representative moment in time. (a–d) The velocity with the low wavenumbers ( $k < k_{fil}$ ) filtered off for (a)  $k_{fil} = 200$ , (b) 10, (c) 1, and (d) 50. (e–h) The velocity with the high wavenumbers ( $k > k_{fil}$ ) filtered off for (e)  $k_{fil} = 200$ , (f) 10 and (g) 1.



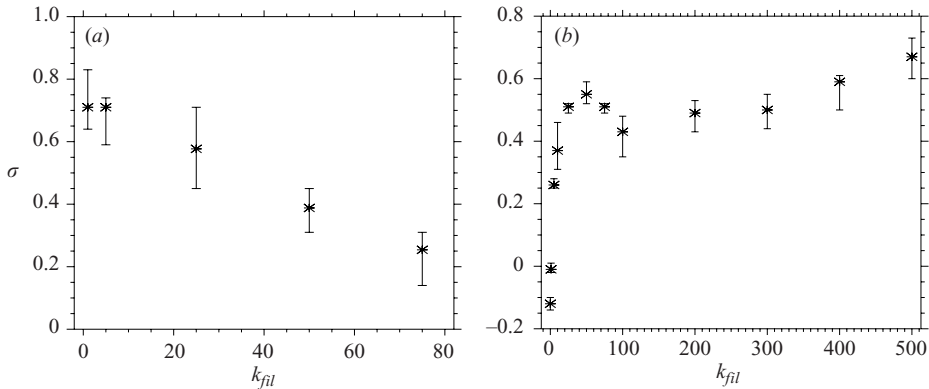


FIGURE 9. growth rate  $\sigma$  versus  $k_{fil}$ . (a) The case where the large-scale modes ( $k < k_{fil}$ ) are filtered off; (b) the case where the small-scale modes ( $k > k_{fil}$ ) are filtered off. The error bars indicate the maximum and minimum growth rates over intermediate sub-intervals of the exponential growth.

are kept and the high wavenumbers are filtered off. This figure should be read from the right. For high  $k_{fil}$  the velocity field is largely unaffected and the growth rate remains that for the full velocity field. As  $k_{fil}$  is decreased, more and more modes are filtered out, but this has a very small effect on the growth rate for a large range of values of  $k_{fil}$  ( $30 \lesssim k_{fil} \lesssim 600$ ) – it is only when the filter acts to remove the ‘active dynamo scales’ at  $k_{fil} \approx 20$ – $30$  that the growth rate drops significantly. This result deserves some immediate discussion. For the full velocity we demonstrated earlier that the diffusive cutoff for the magnetic field lay in the inertial range of the turbulent velocity field. The dynamo therefore corresponded to one operating at low magnetic Prandtl number  $Pm$ . As the velocity field becomes successively more filtered, the cutoff moves to large scales and eventually lies significantly to the left of the resistive cutoff for the magnetic field. At this point the dynamo corresponds to one operating at high magnetic Prandtl number  $Pm$ , where the velocity is smooth on the scale of the boundary layer for the magnetic field. It is often conjectured that the addition of velocity scales to the right of the dissipative cutoff for the magnetic field will have the effect of switching off the dynamo. This is certainly not the case here and dynamos at low  $Pm$  will therefore work just as efficiently as those at high  $Pm$  providing that the ‘active dynamo scales’ (i.e. scales in the turbulent velocity where  $Rm > Rm_c$ ) are still present in the turbulent cascade. We shall return to this point in the discussion.

The effects of filtering the velocity are also apparent in the form of the magnetic field, as shown in figure 10. This shows  $B_x$  for the case when the high wavenumbers are filtered off (i.e. this is the case corresponding to the velocities in figure 8a–d). For high values of  $k_{fil}$ , where the velocity field and growth rate do not differ significantly from those for the full velocity, the magnetic field (figure 10a, b) unsurprisingly is similar to that for the full velocity with strong magnetic fields appearing in filaments around the eddies with a size determined by the active dynamo scale. When the active eddies are removed by filtering, however, the magnetic field takes on a rather different form, shown most clearly in figure 10(d). Here the magnetic field still takes the form of filamentary structures, but now these appear in bands that have a typically larger length scale associated with them. The relative size of the magnetic filaments to these bands of magnetic field is now small, with many thin filaments of oppositely directed field making up a band. This structure of the field can be well understood within the

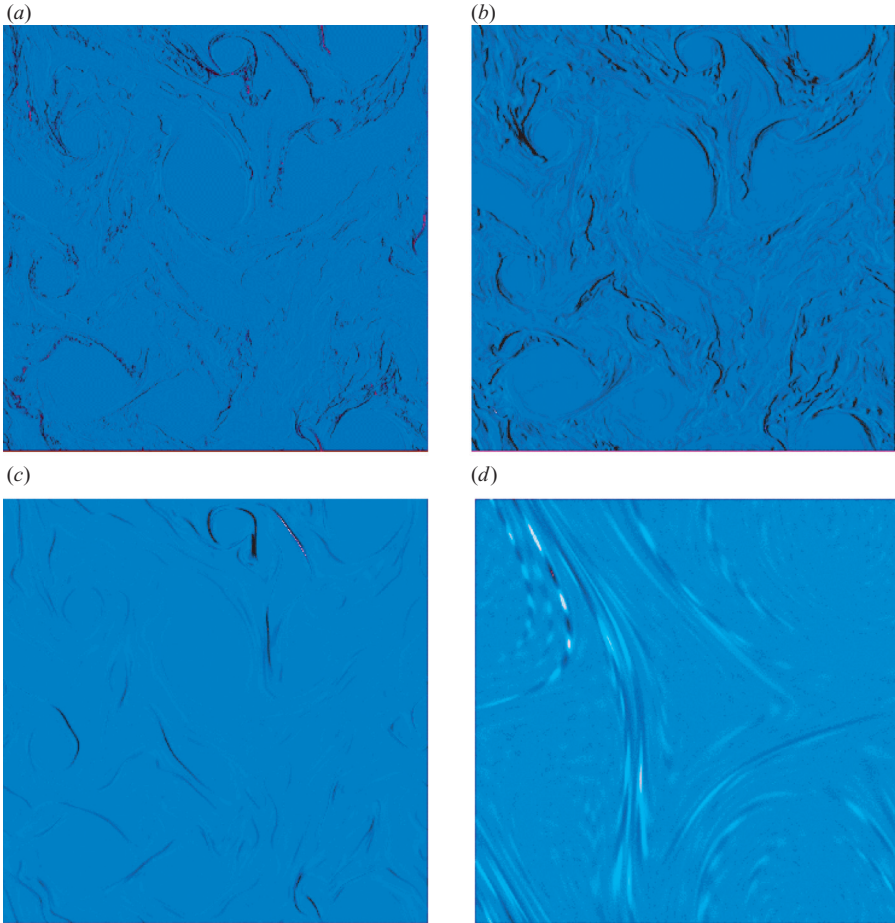


FIGURE 10. Density plots of the magnetic field  $B_x$  for the cases shown in figure 8(e–h).

framework of the theory. As the active wavenumbers are excluded from the velocity field by the filtering, the length scales in the velocity that are important for the dynamo move to larger values – hence the bands of magnetic field are associated with large scales. These larger-scale eddies (although slow) are at high  $Rm$  so any filamentary magnetic field associated with them will be on a fine scale.

At this point we note that the arguments above are complicated somewhat by the fact that in all of the filtering we have kept the wavenumber  $k_z$  at a fixed value. Of course in reality the results should be optimized over all  $k_z$  to be compared with fully three-dimensional magnetic fields. Indeed one may expect that as the velocity is filtered the preferred value of  $k_z$  will change somewhat, as described in the discussion. However it is no simple task to perform these calculations (which require significant resources) at a wide range of  $k_z$  and this is beyond the scope of this paper. Moreover, the fact that these calculations were performed at low values of  $\eta = 0.0001$  and therefore high  $Rm$  reduces the sensitivity to  $k_z$  with many values of  $k_z$  having similar growth rates.

What we have shown above is therefore that there does appear to be a range of wavenumbers that is largely responsible for the generation of magnetic field in this flow. The proposition of § 2 is that these wavenumbers can be identified as the fastest

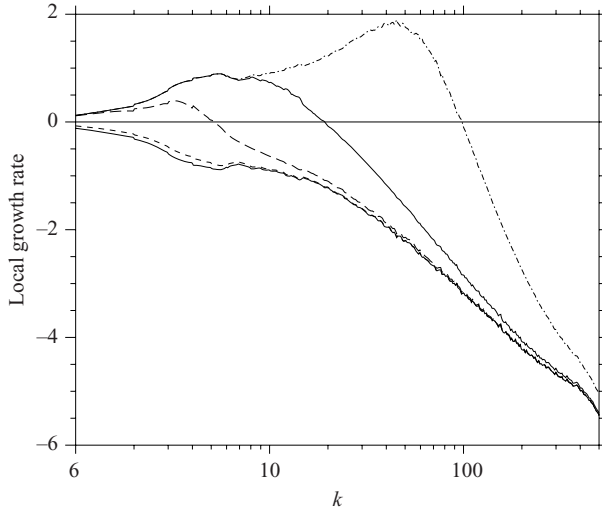


FIGURE 11. ‘Local growth rate’  $\sigma_{loc}$  as a function of  $k$  for  $\eta = 0.01, 0.001$  and  $0.0001$ . In each case the local  $Rm$  and  $\tau$  are calculated from the spectrum (given in figure 4a) and the local growth rate is found by employing the formula in equation (2.5).

eddies for which  $Rm$  is greater than its critical value. In that section we identified the ‘active wavenumbers’ by assuming a given power-law spectrum for the turbulence and a typical form for the growth curve as a function of  $Rm$ . For the turbulent flow analysed here there is no need to assume the form of the spectrum as it has been calculated directly. The ‘active wavenumbers’ can again therefore be identified by determining  $Rm(k)$  and  $\tau(k)$  and assuming a growth-curve dependence of  $\sigma$  on  $Rm$  (such as that used before in equation (2.5) and shown in figure 1). The results are shown in figure 11 for three representative values of  $\eta$ . As  $\eta$  is decreased the band of ‘active wavenumbers’ increases and the maximum growth rate moves to higher values of  $k$ . For the two smallest values of  $\eta$  the preferred wavenumbers are in the range  $10 \lesssim k \lesssim 100$ , consistent with the value found by the filtering. We stress again that the process here is sensitive to the precise form assumed for the growth curve as a function of  $Rm$ , but computations with different (realistic) forms of the growth curve identify similar scales as being important for dynamo action. Hence we are confident that the numerical results are consistent with the scenario proposed in §2.

## 7. Conclusions

In this paper we have presented a theory for the behaviour of kinematic dynamos driven by complex flows consisting of a spectrum of eddies and a hierarchy of coherent structures. This theory identifies the spatial scales that are important for dynamo action and leads directly to the growth of magnetic field. The theory is derived by considering each scale acting as a dynamo in isolation; at each scale the growth rate of the associated magnetic field is a function both of the local  $Rm$  for the eddy and the local turnover time  $\tau_c$ . Because both the local magnetic Reynolds number and the turnover time are increasing functions of spatial scale the dynamo growth is then determined by a competition between large (high  $Rm$ ) slow (large  $\tau_c$ ) eddies and small (low  $Rm$ ) fast (small  $\tau_c$ ) eddies. We propose that the dynamics is then often controlled by eddies on an intermediate scale where the local magnetic

Reynolds number is close to the critical  $Rm$  for the onset of dynamo action at that scale. We identify this scale as the ‘active dynamo scale’. It is now apparent that for flows in a turbulent spectrum the dynamo properties are set by the behaviour of the local growth curve for a value of  $Rm$  just above critical. It is therefore useful to introduce the concept of a ‘quick dynamo’; this is a dynamo where the growth rate reaches a large fraction of its maximum value for  $Rm \sim Rm_c$ . We note again here that a dynamo may be ‘quick’ whether it is fast or slow! The definition of quick does not take into account the behaviour of the growth rate at large  $Rm$ . If the eddies in isolation act as quick dynamos (which we believe to be the generic case) then the identification of a sharp band of active dynamo scales in the turbulent spectrum is possible.

In order to test the applicability of the above theory, we conducted a systematic investigation of the dynamo properties of a range of turbulent flows that consisted of a spectrum of coherent eddies. The flows were constructed to be 2.5-dimensional and with the property that the spectral slope was a function of a ‘localization parameter’  $\lambda$ . The nature of the flows chosen and the use of massively parallel computers facilitated the investigation of the dynamo properties for extreme values of the parameters. For example, both the fluid and magnetic Reynolds numbers can be chosen to be extremely large whilst the magnetic Prandtl number can be chosen to be small (so that the dissipative cutoff for the magnetic field occurs in the middle of the inertial range for the turbulence). We find that, as predicted by the theory, the growth of the magnetic field appears to be associated with eddies in the turbulent spectrum of a certain size. The size of these active eddies (and indeed the scale of the associated magnetic field) changes as  $Rm$  is increased, in contrast to fast dynamo studies conducted for velocity acting at one scale (e.g. Galloway & Proctor 1992) where the scale of the field remains fixed as  $Rm$  changes. We also note that the flows remain efficient kinematic dynamos even when  $Pm \ll 1$ .

As a final test of the theory, the velocity field was then filtered and used as a dynamo in an attempt to identify and isolate the active dynamo scales. Both a high-pass and low-pass filter were used on the velocity. Two interesting results were identified by this procedure. First it allowed the unambiguous identification of the active dynamo scale as predicted by the theory. This occurs at an intermediate scale where the local  $Rm$  is of the same order as  $Rm_c$  and the local turnover time is relatively short. Moreover it was demonstrated, by filtering off the high wavenumbers from the velocity, that the growth rate is not sensitive to whether the dissipative cutoff for the magnetic field is at a larger or smaller scale than that for the velocity (i.e. whether the velocity is rough or smooth on the scale of the magnetic dissipation). The dynamo behaviour is completely controlled by the eddies on the active dynamo scales and it makes little difference to this behaviour whether an inertial range exists at scales smaller than the dissipative cutoff for the field. Thus, dynamo action in a velocity comprising a spectrum of coherent eddies is controlled by the eddies acting on the active dynamo scales which can be identified by examining the competition between large slow eddies and small quick ones.

These findings are particularly relevant to the problem of dynamo action at small values of  $Pm$ . It is useful to distinguish between two cases: one (which has been extensively studied in the past) in which the velocity is mostly random, i.e. it is mostly defined by the inertial-range spectrum; and one, more relevant to astrophysical and geophysical flows, in which long-lived coherent structures are also present, for which this is the first study. In the random case, as shown analytically by Boldyrev & Cattaneo (2004), the determining factor for the critical magnetic Reynolds number

for dynamo action is the roughness exponent of the velocity defined on a range of spatial scales comparable to the scales on which reconnection occurs. According to this picture, as the magnetic Prandtl number decreases through unity, the roughness exponent of the velocity at the relevant dynamo scales changes from unity (smooth velocity) to some value less than unity characteristic of the velocity inertial range. The critical magnetic Reynolds number then shows a corresponding increase. Crucially, once the magnetic Prandtl number is small enough to make the velocity at the dynamo scale rough, further decreases in  $Pm$  have no effect on the critical value of  $Rm$ . These conclusions have been verified numerically by Ponty and collaborators (Ponty *et al.* 2005) who have considered dynamo action with decreasing values of  $Pm$  by constructing the velocities by solving the fully resolved Navier–Stokes equations for moderate values of  $Pm$ , and filtered (momentum) equations for small values of  $Pm$ . As noted in the introduction, studying dynamos in the context of a filtered momentum equation makes the assumption that the small scales in the velocity are unimportant. As predicted by Boldyrev & Cattaneo (2004), the computed value of the critical magnetic Reynolds number increased sharply as  $Pm$  decreases through unity with a subsequent levelling off for smaller values of  $Pm$ . By contrast, in the case in which coherent structures are present, what matters is whether the structures are quick dynamos or not. However, in this paper we have postulated and verified numerically that, just as in the random case, the presence of structures on scales much smaller than the active dynamo scales does not significantly alter the overall dynamo properties.

Finally, we should note that the idea of the fast dynamo limit, in which for a fixed velocity one considers the limit of infinite  $Rm$ , is inconsistent with dynamo action at small  $Pm$ . Once the velocity has been fixed, increasing  $Rm$  is equivalent to increasing  $Pm$ . One could, in principle, consider the abstract case of a velocity field with an infinity spectrum, i.e. one with no high-wavenumber cutoff; in this case, it is clear from the arguments presented above that the growth rate would increase without bounds as  $Rm \rightarrow \infty$ .

## REFERENCES

- BACHELOR, G. K. 1950 On the spontaneous magnetic field in a conducting liquid in a turbulent motion. *Proc. R. Soc. Lond. A* **201**, 405–416.
- BOLDYREV, S. & CATTANEO, F. 2004 Magnetic-field generation in Kolmogorov turbulence. *Phys. Rev. Lett.* **92** (14), 144501.
- BRUMMELL, N. H., CATTANEO, F. & TOBIAS, S. M. 2001 Linear and nonlinear dynamo properties of time-dependent ABC flows. *Fluid Dyn. Res.* **28**, 237–265.
- CATTANEO, F. & TOBIAS, S. M. 2005 Interaction between dynamos at different scales. *Phys. Fluids* **17**, 127105 1–6.
- CONSTANTIN, P., NIE, Q. & SCHÖRGHOFER, N. 1998 Nonsingular surface quasi-geostrophic flow. *Phys. Lett. A* **241**, 168–172.
- GALLOWAY, D. J. & PROCTOR, M. R. E. 1992 Numerical calculations of fast dynamos in smooth velocity fields with realistic diffusion. *Nature* **356**, 691–693.
- HELD, I. M., PIERREHUMBERT, R. T., GARNER, S. T. & SWANSON, K. L. 1995 Surface quasi-geostrophic dynamics. *J. Fluid Mech.* **282**, 1–20.
- KAZANTSEV, A. P. 1968 Enhancement of a magnetic field by a conducting fluid. *Sov. Phys. JETP* **26**, 1031–1031.
- KRAICHNAN, R. H. & NAGARAJAN, S. 1967 Growth of turbulent magnetic fields. *Phys. Fluids* **10**, 859–870.
- LLEWELLYN-SMITH, S. G. & TOBIAS, S. M. 2004 Vortex dynamos. *J. Fluid Mech.* **498**, 1–21.

- MCWILLIAMS, J. C. 1984 The emergence of coherent isolated vortices in turbulent flow. *J. Fluid Mech.* **146**, 21–43.
- OTANI, N. F. 1993 A fast kinematic dynamo in two-dimensional time-dependent flows. *J. Fluid Mech.* **253**, 327–340.
- PARKER, E. N. 1979 *Cosmical Magnetic Fields: Their Origin and their Activity*. Clarendon; Oxford University Press.
- PIERREHUMBERT, R. T., HELD, I. M. & SWANSON, K. L. 1995 Spectra of local and nonlocal two dimensional turbulence. *Chaos, Solitons Fractals* **4**, 1111–1116.
- PONTY, Y., MININNI, P. D., MONTGOMERY, D. C., PINTON, J.-F., POLITANO, H. & POUQUET, A. 2005 Numerical study of dynamo action at low magnetic Prandtl number. *Phys. Rev. Lett.* **94**, 164502-1–4
- PONTY, Y., POLITANO, H. & PINTON, J.-F. 2004 Simulation of induction at low magnetic Prandtl number. *Phys. Rev. Lett.* **92**, 144503-1–4
- ROBERTS, G. O. 1972 Dynamo action of fluid motions with two-dimensional periodicity. *Phil. Trans. R. Soc. Lond. A* **271**, 411–454.
- SAFFMAN, P. G. 1963 On the fine-scale structure of vector fields convected by a turbulent fluid. *J. Fluid Mech.* **16**, 545–572.
- SCHEKOCHIHIN, A. A., COWLEY, S. C., MARON, J. L. & MCWILLIAMS, J. C. 2004 Critical Magnetic Prandtl Number for Small-Scale Dynamo. *Phys. Rev. Lett.* **92** (5), 054502–+.
- SCHEKOCHIHIN, A. A., HAUGEN, N. E. L., BRANDENBURG, A., COWLEY, S. C., MARON, J. L. & MCWILLIAMS, J. C. 2005 The onset of a small-scale turbulent dynamo at low magnetic Prandtl numbers. *Astrophys. J.* **625**, L115–L118.
- THOMSON, D. J. & DEVENISH, B. J. 2005 Particle pair separation in kinematic simulations. *J. Fluid Mech.* **526**, 277–302.
- VAINSHTEIN, S. I. & KICHATINOV, L. L. 1986 The dynamics of magnetic fields in a highly conducting turbulent medium and the generalized Kolmogorov-Fokker-Planck equations. *J. Fluid Mech.* **168**, 73–87.
- ZEL'DOVICH, Y. B. 1957 The magnetic field in the two dimensional motion of a conducting turbulent liquid. *Sov. Phys. JETP* **4**, 460–462.